Polypropylene Surface Modification in Atmospheric Pressure Dielectric Barrier Discharges (DBD).

S. Guimond[a], I. Radu[a], G. Czeremuszkin[b], D.J. Carlsson[c], and M.R. Wertheimer[a]*

a: Groupe des Couches Minces (GCM), Department of Engineering Physics and Materials Engineering, Ecole Polytechnique, Montreal (Quebec), Canada.
b: Polyplasma Inc., Montreal (Quebec), Canada.
c: National Research Council of Canada, Institute for Chemical Process and Environmental Technology, Ottawa (Ontario), Canada.

*corresponding author; e-mail: mwertheimer@ courriel.polymtl.ca

Abstract

We compare two surface treatments of biaxially-oriented polypropylene (BOPP) carried out in the same dielectric barrier discharge (DBD) apparatus, namely air corona, and N_2 atmospheric pressure glow discharge (APGD). It is shown that the latter treatment leads to a higher surface energy than the former, and to the formation of mostly amide and amino groups.

1. Introduction

Modifying polymer surfaces by plasmas is of great industrial relevance (1). However, most of the methods currently used have significant disadvantages. With in-line corona treatment in air, for instance, the extent of achievable surface modifications is limited, since bond scission rapidly sets in during oxidation, which results in the formation of so-called "low molecular weight oxidized materials" (LMWOM) (2). Hence, air-corona treatments permit only a limited surface oxidation chemistry. On the other hand, low-pressure plasma treatment requires expensive vacuum systems and batch processing. With these considerations in mind, it now appears that a possible compromise solution can be provided by so-called atmospheric pressure glow discharge (APGD) processes, the focus of this communication. Numerous recent reports have confirmed that a "glow" (non-filamentary) discharge can be obtained at atmospheric pressure in helium and in nitrogen (3-10). This type of discharge is generally created between two parallel plane electrodes at high voltage and at frequencies in the multi-kilohertz range. The configuration used is that of a dielectric barrier discharge (DBD); that is, at least one of the electrodes is covered with a dielectric, as in the case of corona systems. It has been shown that the "APGD" regime reverts to a filamentary discharge if a certain concentration of impurities in the gas is exceeded (11). To avoid this problem, it is therefore necessary to carefully control the composition of the gas fed into the discharge. Thus, several authors have studied the discharge behavior or its interaction with polymers in closed vessels that could be evacuated prior to the experiments (5-12). However, from an industrial point of view, the evacuation of the system prior to introducing the process gas does not have a practical and economical advantage over the use of low-pressure plasma systems.

In the present paper, we first describe a system for continuous APGD treatment of polymer films that does not require prior evacuation. We then present preliminary results of a systematic study of nitrogen (N_2) APGD treatment of biaxially-oriented polypropylene (BOPP) in our pilot-scale facility. Changes in the surface energy and in the surface chemistry are examined as a function of the energy dose, E_d, (in J/cm^2) of treatment. The results are compared with those obtained by air corona, using the same DBD apparatus.

2. Experimental methodology

Treatment conditions

The polymer used in this study is a commercial, melt-extruded and biaxially-oriented polypropylene film (BOPP). No oxygen was detected by XPS on the untreated film surface. Using the method of Owens and Kaelble (13), a surface energy of 27±1 dynes/cm has been measured for the untreated film. The very same material has previously been used by other authors for studies on the effect of corona treatment (2, 14, 15).

The DBD experimental setup, which has been used for both N_2 APGD and corona treatments, is presented schematically in Fig. 1. It consists of a 24 x 29 cm grounded Al plate electrode, that can be moved at precisely controlled speed under the cylindrical, high-voltage electrode. Two dielectrics have been used here: the grounded electrode was covered with a 2 mm thin borosilicate glass plate (on which the polymer reposed), while the high-voltage electrode was covered with a 0.36 mm plasma-sprayed layer of alumina + 13% TiO_2 (11).

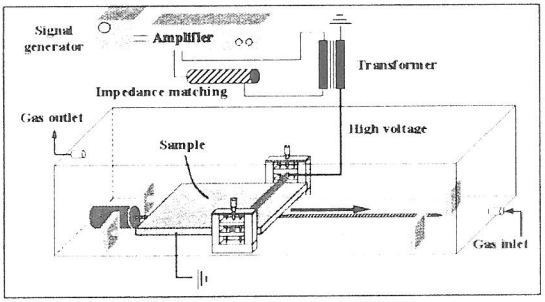

Figure 1. Schematic view of the DBD treatment facility

An inter-electrode gap of 1 mm has been used throughout this study. The system is housed in an airtight Plexiglass enclosure, which is continuously flushed with a 9 slm flow of the desired treatment gas (dry air for corona, and UHP-grade nitrogen for APGD). As previously mentioned, to avoid contamination, hence the transition to a filamentary discharge, it was necessary to assure a very low level of impurities in the discharge treatment zone, both from the feed gas and from a build-up of volatile products from the discharge-treated surface. For this purpose, a gas diffuser, which supplies only that region of the system where the discharge is generated, has been built and implemented.

For each treatment, the energy density, E_d, has been calculated using the following formula:

$$E_d = \frac{V_m \cdot I_m \cdot \cos\phi}{w \cdot s} \text{ (J/cm}^2\text{)},$$

where ($V_{rms} \cdot I_{rms} \cdot cos\ \phi$) is the electrical power dissipated in the gas (in W), w is the width of the discharge zone (24 cm), and s is the effective speed of the moving electrode (cm/s). In turn, $s = l/t$, where l is the "length" of the discharge zone (~1cm) and t is the residence time. In this study, a single discharge frequency, f = 1 kHz, has been used for both corona and N_2 APGD treatments. This is well below the typical frequency values used for industrial corona treatments (f~20 kHz); in future work, the effect of this important parameter, f, will be examined. To establish whether the discharge is of the glow or the filamentary type, the method previously described by Miralaï et al has been used (11): it consists of simultaneously measuring the discharge current waveform and the photomultiplier signal of light emitted from the gap.

Surface analysis

After each treatment, the polymer was analyzed by XPS (less than 5 hours after the treatment) and by contact angle goniometry with several probe-liquids, using the method of Owens and Kaelble (13) (typically, within 30 minutes after the treatment). This latter method allowed us to determine the polar (γ_s^{pol}) and dispersive (γ_s^{disp}) components of the polymer's surface energy, γ_s. The liquids used are water, glycerol, formamide, ethylene glycol, and tricresylphosphate. XPS analyses were performed in a VG ESCALAB 3MkII system, using non-monochromatic Mg Kα radiation. Spectra were acquired at a take-off angle normal to the sample surface, and the binding energies were referenced to the carbon (C1s) peak at 285.0 eV, to adjust for possible charging effects. Some samples treated at high values of E_d were also analyzed by Fourier-transform infrared spectroscopy (FTIR), using the attenuated total reflectance (ATR) technique at 45° incidence, with the help of a germanium crystal (a 45°-facet angle, Single Pass Trapezoid Plate, from Harrick Scientific Corporation).

3. Results and discussion

Surface energy

For the case of nitrogen APGD treatments, γ_s increases with increasing E_d, and it appears to saturate near 57 dynes/cm, for E_d = 6.3 J/cm^2. For corona treatments, γ_s again increases with increasing E_d, but saturates near 40 dynes/cm, for an applied dose (E_d) below 0.1 J/cm^2. It is, therefore, possible to affirm that nitrogen APGD can lead to a higher degree of surface activation than air corona, although γ_s at saturation appears to require a higher E_d value. It is also noteworthy that for both treatment types, the observed increase in γ_s appears to be entirely due to changes in the polar component, γ_s^{pol}, which is initially zero for the untreated BOPP surface. This latter component results from the creation of polar chemical groups during the treatment, as is shown below.

XPS analyses

In Fig. 2, the evolution of the concentrations of bonded oxygen and nitrogen with increasing treatment doses are shown plotted for the cases of air corona and nitrogen APGD, where the relative atomic percentages have been determined by XPS. Only oxygen is chemically incorporated into the polymer surface after air corona treatments, while in the case of N_2 APGD, both bonded nitrogen and oxygen are encountered. The presence of oxygen in the latter case must be due to post-treatment reactions, when the sample is exposed to ambient atmosphere; at this time, long-lived free radicals or unstable functional groups near the surface can react with molecular oxygen or water vapor (16).

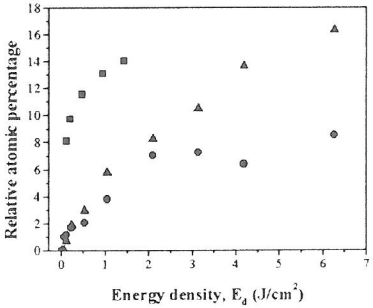

Figure 2. Surface concentrations of bonded oxygen and nitrogen, plotted as a function of the corona and nitrogen APGD energy densities (doses), E_d; ■ [O] after air corona; ▲ [N] and ● [O] after nitrogen APGD.

A deeper insight into the APGD-treated polypropylene surface chemistry has been made possible by the combined use of high-resolution XPS and ATR-FTIR (see next section for the latter). The results of the C1s, O1s and N1s peak deconvolutions and their assignments are summarized in Table 1, for a nitrogen APGD-treated BOPP sample (E_d = 6.3 J/cm^2). From the high-resolution XPS analysis, we can conclude that the N_2 APGD treated BOPP surface contains carbon atoms that are singly- or doubly-bonded to oxygen, and carbon atoms that are mostly singly- (but some multiply-) bonded to nitrogen (16). Finally, amide groups (N-C=O) may also be present. We can exclude the appreciable presence of nitro (C-NO_2), oxime (C=NOH) and nitrate (C-ONO_2) groups, since no major shift is observed in the N1s peak. For more specific identification of chemical functional groups, we have compared this XPS analysis with the infrared spectroscopy results, given below.

Infrared analyses

The ATR-FTIR spectrum of a virgin BOPP sample (not shown, for lack of space) shows a series of peaks between 2950 and 2800 cm^{-1}, which correspond to the various aliphatic CH stretching modes. Another series of peaks near 1450 cm^{-1} and 1380 cm^{-1} are the CH_2 and the CH_3 deformation bands, respectively. Other peaks below 1300 cm^{-1} are the well-known "fingerprint" of isotactic PP. The difference spectrum (untreated sample spectrum subtracted from the treated sample spectrum) of a 9.4 J/cm^2 N_2 APGD-treated BOPP sample is depicted in Fig. 3(a), in which arrows mark the positions of new peaks; Fig. 3(b) is the difference spectrum of a 2.9 J/cm^2 air corona-treated BOPP sample. The most plausible peak assignments are summarized in Table 2, whereby we have excluded certain chemical groups, based on the results of the foregoing high-resolution XPS analyses.

The carbonyl (C=O stretch) IR band is intense in the case of oxidized polymer surfaces, as can be seen from Fig. 3(b); it possibly comprises carboxylic acid (between 1710 and 1690 cm^{-1}), ketone (between 1720 and 1700 cm^{-1}), ester (between 1750 and 1740 cm^{-1}) and aldehyde (between 1740 and 1720 cm^{-1}) C=O stretching bands. These are either absent, or in low concentration in the N_2 APGD sample.

From the two complementary analytical data sets, we conclude that amines and amides are present after N_2 APGD treatment.

Table 1. The results of high resolution XPS C1s, O1s and N1s peak deconvolutions and their assignments. N_2 APGD-treated polypropylene, E_d = 6.3 J/cm^2.

	Peak	Center (eV)	Δ B.E (eV)	Assignment	%Area
C1s	1	-285.0	0	C-H, C-C	68.54
	2	-285.9	0.9	C-N, C-O	15.18
	3	-286.7	1.7	C=N	2.13
	4	-287.6	2.6	N-C=O, C=O	8.78
	5	-288.9	3.9	N-C-N, O-C=O O	5.38
O1s	1	-531.5	-	C=O	59.68
	2	-532.7	-	C-O	40.32
N1s	1	-399.2	-	C-N	45.66
	2	-400.5	-	N-C=O, C=N, C≡N	54.34

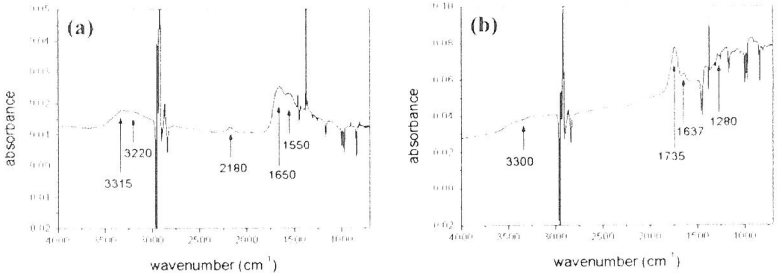

Figure 3. (a) ATR-FTIR difference spectrum of a N_2 APGD-treated BOPP sample (E_d = 9.4 J/cm^2). (b) ATR-FTIR difference spectrum of an air corona-treated BOPP sample (E_d = 2.9 J/cm^2). Both spectra are not ATR depth corrected (200 spectra co-added; the resolution is 4 cm^{-1}).

Table 2. Assignments of the new infrared absorbance bands observed in the spectrum of a 9.4 J/cm^2 N_2 APGD-treated and a 2.9 J/cm^2 air corona-treated BOPP sample.

	Wavenumber (cm^{-1})	Assignment
N_2 APGD	3300-3200	OH, NH stretch
	2180	N≡C stretch
	1650	C=C stretch, C=N stretch, C=O stretch in amides, NH_2 deformation in primary amines
	1550	NH_2 and NH deformations in amides

Air corona	3300	OH stretch
	1735	C=O stretch (carboxylic acids, ketones, esters and aldehydes)
	1637	C=C stretch
	1280	C-O-C stretch

Other unsaturated species such as C=C, C≡N and C=N may well also be formed, but require further confirmation. In order to more precisely identify the nature of the functional groups created, and to determine their relative concentrations, the use of chemical derivatisation schemes and of time of flight secondary ion mass spectrometry (ToF-SIMS) are now in progress in this laboratory. This also applies to a study of "aging" of treated materials.

4. Conclusions

We have demonstrated treatment of polymer films in a continuous process by nitrogen APGD, in a system that does not require prior evacuation. N_2 APGD treatments can raise γ_s of BOPP to significantly higher values than those achievable with air corona treatments. We have also determined, by high-resolution XPS and by ATR-FTIR, that the principal chemical functional groups created on BOPP surfaces by N_2 APGD treatments are amines and amides, while air corona-treatment leads only to the formation of oxidized carbon (hydroxyls, ketones, etc).

5. Acknowledgments

This work constitutes part of the scientific program of the NSERC Industrial Research Chair on Plasma Processing of Materials. The authors wish to thank Dr J.E. Klemberg-Sapieha for useful discussions and for help with XPS analyses, and Dr Mark Strobel (3M Company, St Paul MN) for kindly providing the BOPP material. They also gratefully acknowledge the expert technical support provided by Mr. Gilles Jalbert.

6. References

1. K.L. Mittal and A. Pizzi (Eds.), *Adhesion Promotion Techniques*, Marcel Dekker Inc., New York, 1999.
2. M. Strobel, C. Dunatov, J.M. Strobel, C.S. Lyons, S.J. Perron and M.C. Morgen, *J Adhesion Sci Technol*, 3(5), 321, 1989
3. R. Bartnikas, *Brit J Appl Phys*, 1, 659, 1968.
4. R. Bartnikas, *IEE Trans Electr Insul*, EI6, 63, 1971.
5. S. Kanazawa, M. Kogoma, T. Moriwaki and S. Okazaki, *J Phys D: Appl Phys*, 21, 838, 1988.
6. N. Gherardi, E. Gat, G. Gouda and F. Massines, *Proc. "Hakone VI"*, Cork, 123, 1998.
7. F. Massines, A. Rabehi, P. Decomps, R. Ben Gadri, P. Ségur and C. Mayoux, *J Appl Phys*, 83, 2950, 1998.
8. F. Massines and G. Gouda, *J Phys D: Appl Phys*, 31, 3411, 1998.
9. E. Monette, MScA thesis, Ecole Polytechnique, Montreal, 1998.
10. E. Monette, R. Bartnikas, G. Czeremuszkin, M. Latrèche and M.R. Wertheimer, *Proc "ISPC 14"*, Prague, 991, 1999.
11. S.F. Miralaï, E. Monette, R. Bartnikas, G. Czeremuszkin, M. Latrèche and M.R. Wertheimer, *Plasmas and Polymers*, 5(2), 63, 2000.
12. F. Massines, R. Messaoudi and C. Mayoux, *Plasmas and Polymers*, 3(1), 43, 1998.
13. D.H. Kaelble, *Physical Chemistry of Adhesion*, ch 5 and 13, Wiley, New York, 1971.
14. J.M. Strobel, M. Strobel, C.S. Lyons, C. Dunatov and S.J. Perron, *J Adhesion Sci Technol*, 5(2), 119, 1991.
15. M. Strobel, C.S. Lyons, J.M. Strobel and R. Kapaun, *J Adhesion Sci Technol*, 6(4), 429, 1992.
16. J.E. Klemberg-Sapieha, O.M. Küttel, L. Martinu and M.R. Wertheimer, *J Vac Sci Technol*, A9 (6), 2975, 1991.